Supplementary Information

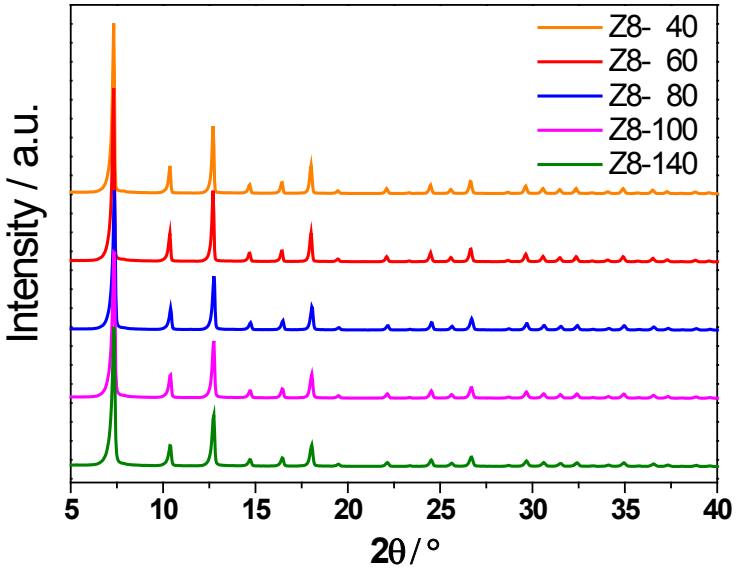

Figure S1. X-ray powder diffraction patterns for Z8-X crystals synthesized with the excess ligand approach in aqueous solution at different ratios, X, of 2-MeIm to Zn(II).

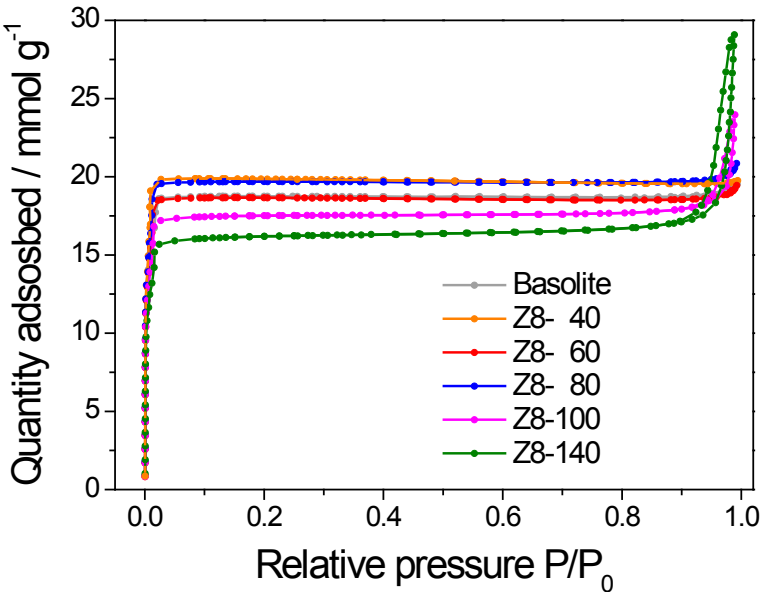

Figure S2. Nitrogen sorption isotherms for Z8-X crystals synthesized with the excess ligand approach in aqueous solution at different ratios, X, of 2-MeIm to Zn(II), and for the commercial Basolite® (Sigma Aldrich, St. Louis, MO, USA), sample.

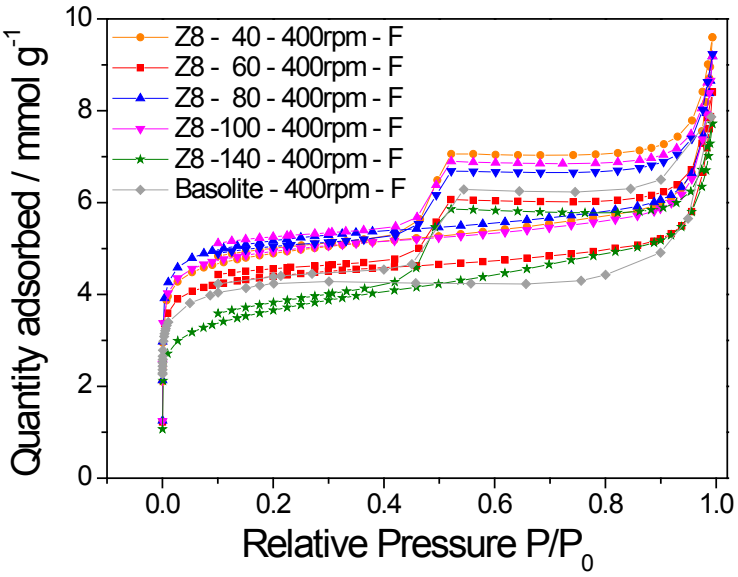

Figure S3. Nitrogen sorption isotherms for the series of Fe–N–C catalysts obtained after milling the precursors at 400 rpm and pyrolyzing them in flash mode at 1050 °C in Ar for 1 h.

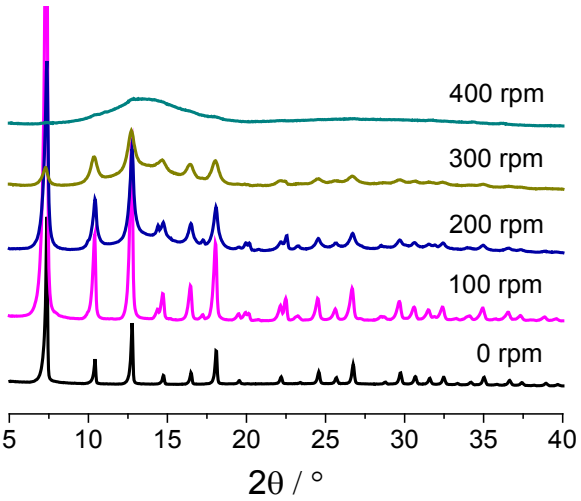

Figure S4. X-ray powder diffraction patterns of Z8-100 milled at different rotation speed.

Z8-100-100 rpm-F

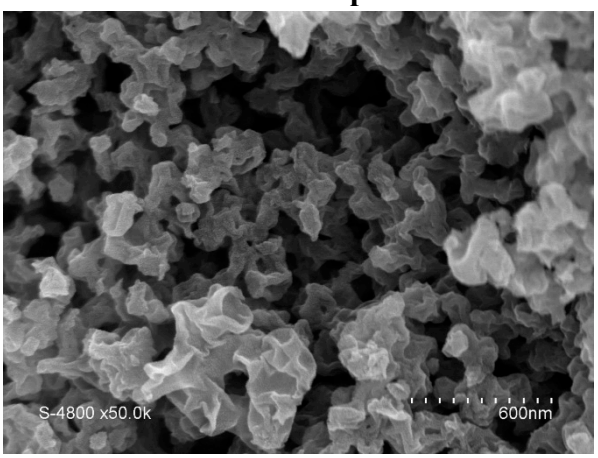

Z8-100-100 rpm-R

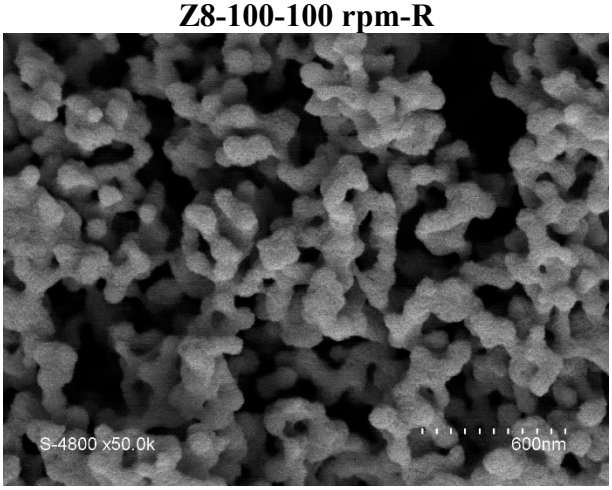

Figure S5. *Cont.*

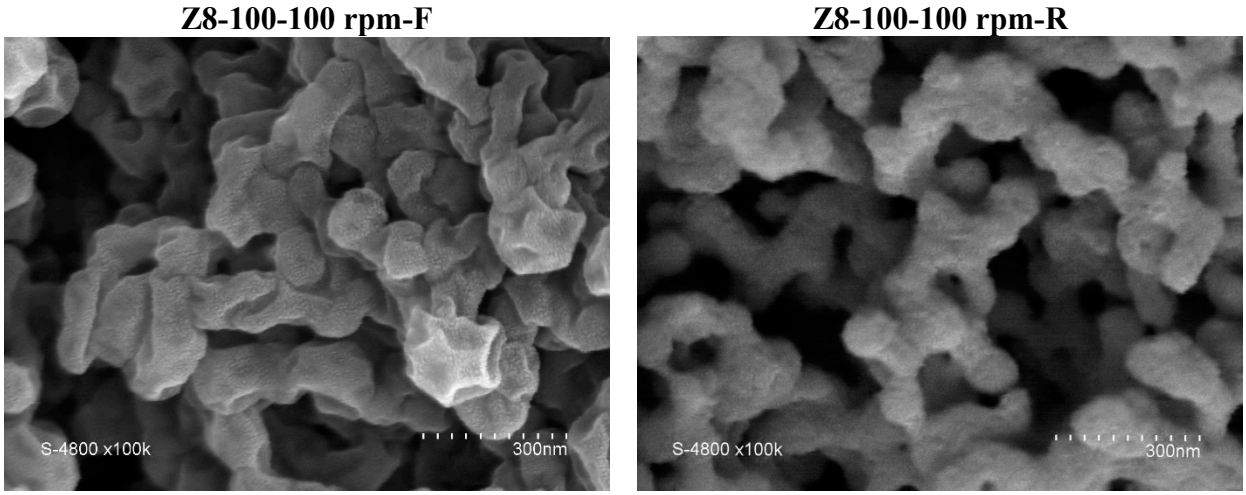

Figure S5. SEM micrographs of two Fe–N–C catalysts obtained after milling the precursors FeAc, phen and Z8-100 at 100 rpm and pyrolyzing them at 1050 °C in Ar in flash mode (F, **left handside**) or ramp mode (R, **right handside**). The scale bar is 600 nm on top and 300 nm on the bottom.

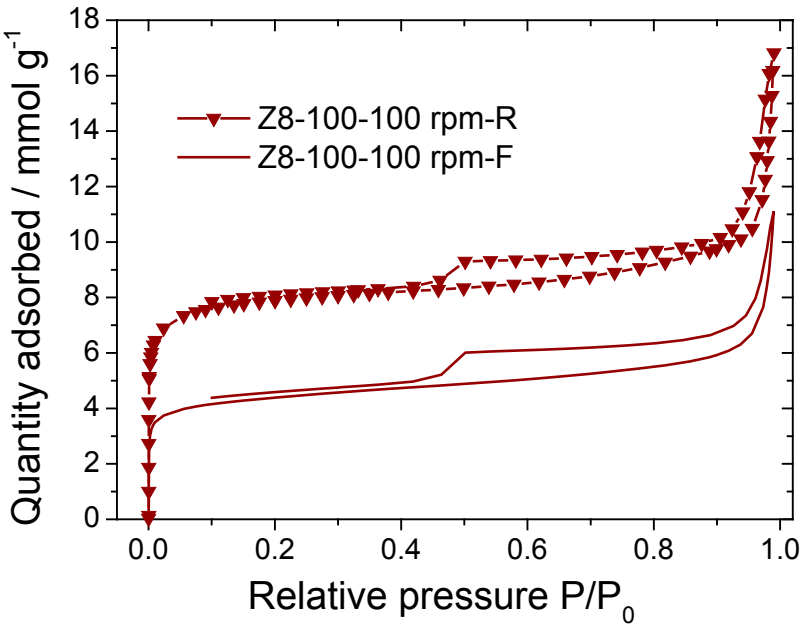

Figure S6. Comparison of N_2 sorption isotherms for two Fe–N–C catalysts pyrolyzed in flash or ramp mode. Ballmilling was carried out at 100 rpm for forming catalyst precursors from Fe(II) acetate, phen and Z8-100, catalyst precursors that were subsequently pyrolyzed in flash (F) or ramp mode (R) at 1050 °C in Ar.

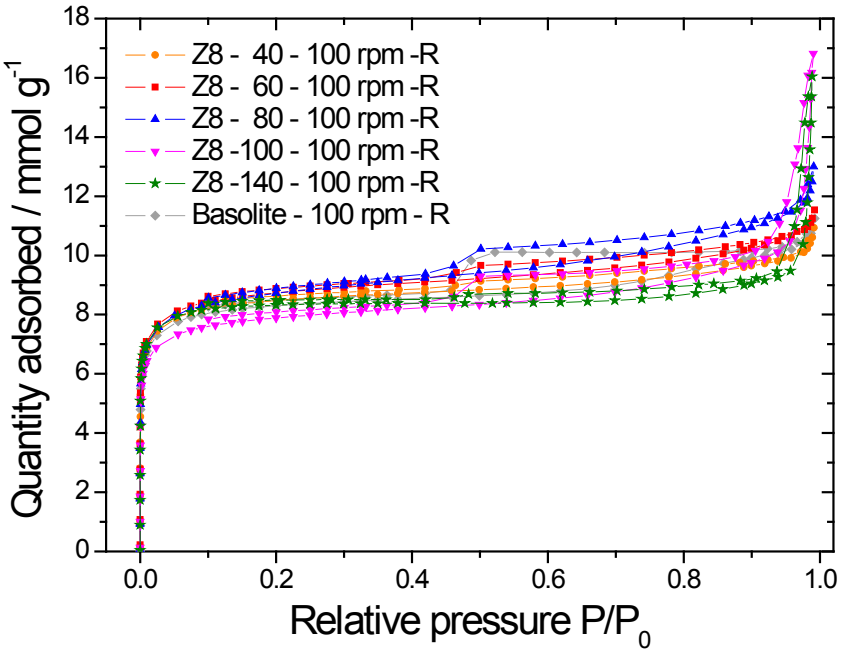

Figure S7. Nitrogen sorption isotherm for the series of Fe–N–C catalysts obtained after milling the precursors at 100 rpm and pyrolyzing them in ramp mode at 1050 °C in Ar.

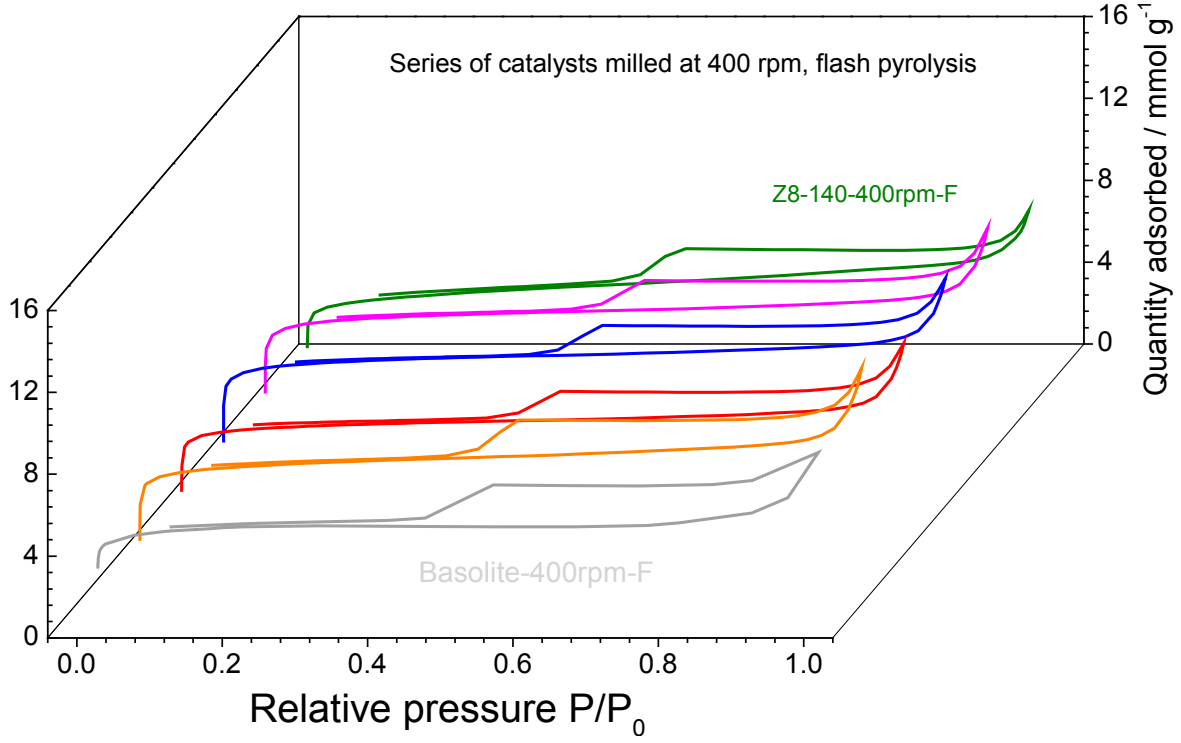

(a)

Figure S8. *Cont.*

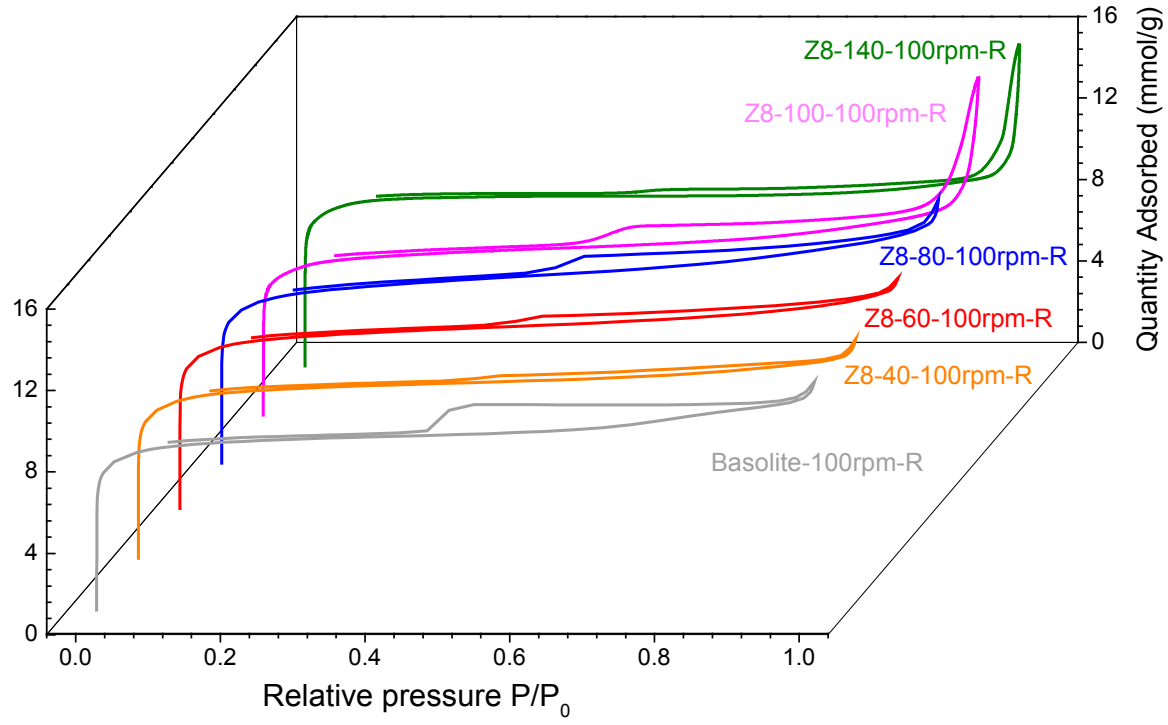

(**b**)

Figure S8. Waterfall comparison of the N_2 sorption isotherms for the first series of Fe–N–C catalysts obtained after 400 rpm milling and flash pyrolysis (**a**) and the second series of Fe–N–C catalysts obtained after 100 rpm milling and ramp pyrolysis; (**b**). The raw data are the same as those shown in Figures S3 and S7.